SCIENCE CHINA Information Sciences



RESEARCH PAPER

 $\begin{array}{c} {\rm January~2026,~Vol.~69,~Iss.~1,~112303:1-112303:14} \\ {\rm ~https://doi.org/10.1007/s11432-025-4446-2} \end{array}$

A tactile codec based on perceptual deadband and differential encoding for tactile Internet

Qi ZHANG, Shengyu ZHANG & Tao JIANG*

Research Center of 6G Mobile Communications, School of Cyber Science and Engineering, Huazhong University of Science and Technology, Wuhan 430074, China

Received 13 January 2025/Revised 5 April 2025/Accepted 14 May 2025/Published online 25 September 2025

Abstract Tactile Internet (TI) introduces tactile feedback to traditional audio-visual feedback for a more immersive user experience in virtual or real environments. Since vibrotactile and force-tactile feedback is the widely experienced tactile feedback in the physical world, efficient transmission of vibrotactile and force-tactile signals is critical for TI. To this end, this work presents a versatile tactile codec based on perceptual deadband and differential encoding, called TC-PDDE, for high-efficiency and low-delay compression of both vibrotactile and force-tactile signals by balancing the reduction of packet size and the decrease of packet rate in tactile communication. First, we adopt a perceptual deadband in the perceptual property to convert original signals into perceptible signals by discarding imperceptible tactile signals. After that, we design a non-uniform quantizer based on the statistical property to quantize and encode the differential compensations of perceptible signals. Finally, we validate the performance of the proposed codec by comparing it with the popular codecs on the standard vibrotactile and self-built force-tactile datasets. The comparison results show that TC-PDDE achieves higher compression efficiency and lower codec delay than other codecs, indicating that TC-PDDE is the superior alternative for real-time tactile applications in TI.

Keywords tactile Internet, tactile communication, vibrotactile, force-tactile, tactile codec

Citation Zhang Q, Zhang S Y, Jiang T. A tactile codec based on perceptual deadband and differential encoding for tactile Internet. Sci China Inf Sci, 2026, 69(1): 112303, https://doi.org/10.1007/s11432-025-4446-2

1 Introduction

Tactile Internet (TI) with Human-in-the-Loop provides an emerging communication paradigm to facilitate the exchange of skills between humans and machines over distances by transmitting tactile information [1]. The applications of TI extend to various scenarios, such as tele-operation [2,3], smart industries [4,5], smart city [6,7], augmented/virtual reality [8], and eHealth [9], with the assistance of high-performance wireless networks [10,11]. To ensure that humans can access the immersive real-time tactile experience and skills can be exchanged efficiently in the applications of TI, tactile information should be processed with lossless perception and low delay [12].

The tactile information is related to the perception of surface properties, including hardness, thermal conductivity, friction force, pressure force, and micro-/macro-roughness [13]. In the above multimodal information, force-tactile information that reflects hardness and vibrotactile information that reflects roughness are currently attracting the most attention, since force-tactile and vibrotactile feedback plays an important role in improving the efficiency and accuracy of tele-operation tasks in TI [14]. Although the transmission of force-tactile and vibrotactile information in the single-point interaction scenarios requires low bandwidth in tactile communication. Given that the skin serves as a sensory organ that covers the entire body, the immersive force-tactile and vibrotactile experiences involving multiple-point interactions may require thousands of parallel tactile information channels [15], which can quickly overwhelm the local networks as well as the long-distance transmission links [12]. Therefore, the tactile codec, which can efficiently compress and reconstruct force-tactile and vibrotactile signals, is critical to alleviate the burden on tactile communication and provide immersive user experiences in TI.

At present, numerous tactile codecs that specialize in the processing of force-tactile information or vibrotactile information have been investigated. In these codecs, an encoder at the transmitting end eliminates redundant information in the time or frequency domain to achieve data compression, and the decoder at the receiving end follows the inverse procedure of the encoder to recover the compressed data. Generally, the available tactile codecs mainly belong to two categories: perception-based tactile codecs and transform-based tactile codecs.

 $[\]hbox{$*$ Corresponding author (email: tao.jiang@ieee.org)}\\$

The perception-based tactile codecs are devoted to reducing the packet rate in tactile communication, which utilizes the limitations of human perception to discard the imperceptible tactile data. The perceptual deadband is one of the important perceptual properties in human psychophysics [16] and has been widely used to compress tactile data while preserving the perception-lossless experience. Hinterseer et al. [17] presented a perception-based data reduction approach to reduce the packet rate of tactile data while maintaining the perception-lossless experience. IEEE P1918.1.1 Haptic Codecs Task Group has developed the standards of perceptual deadband (PD)-based compression scheme to compress force information for TI [18]. By combining dead-zone coding with segmented linear prediction, Xu et al. [19] proposed an improved force-tactile coding algorithm. Liu et al. [20] introduced the perceptual property to compress the vibrotactile and proposed a data-driven approach, in which a compression function designed by data-driven optimization was applied to vibrotactile data and 75% compression of vibrotactile data is achieved. In addition, research in [21] discovered the masking effect in the perception over wideband vibrotactile signals, and presented a bitrate scalable tactile texture codec in combination with the perception masking model.

The transform-based tactile codecs aim to decrease the packet size in tactile communication, eliminating redundant information in the frequency domain. The discrete cosine transformation (DCT) method and its variants have been widely adopted for compressing force data and vibrotactile data [22–24]. Kuzu et al. [25] used the wavelet packet transform (WPT) and the inverse WPT for the coding and decoding operations of tactile data compression. Baran et al. [26] discussed the DCT, discrete Fourier transform (DFT), and WPT-based compression schemes, and then proposed a superior tactile data codec algorithm, namely the selected DCT, integrating the best features of wavelets and DCT transformation. To further reduce coding delay, Zeng et al. [27] developed an end-to-end tactile codec consisting of the amplifier, DCT, quantizer, run-length encoder, and entropy encoder for the compression of tactile signals. Hassen et al. [28] presented a vibrotactile codec scheme that includes the sparse linear predictor and perceptual compressor, where the prediction residuals in the DCT domain were processed by the human tactile sensitivity function. Based on [28], Hassen et al. [29] recommended the tactile sensitivity model ASF (acceleration sensitivity function) to quantify the predicted residuals in the DCT domain. Noll et al. [30, 31] developed and improved a hybrid codec using the discrete wavelet transform (DWT), tactile perception modeling, quantization, and entropy coding.

In addition, several researchers have attempted to develop tactile codecs using deep neural network models. Liu et al. [32] utilized a stacked auto-encoder and gated recurrent units to compress force-tactile signals into compact representations for transmission. Deng et al. [33] suggested a long short-term memory-based mathematical model that combines force data and perceptual deadband for joint training, focusing on the reduction of tactile data without loss of transparency. Zhao et al. [34] developed a vibrotactile codec based on the recurrent network using gated recurrent units, which substantially reduces bitrates with minimal perceptual degradation. Xu et al. [35] presented a Nbeats network-based vibrotactile codec that takes advantage of the statistical properties of vibrotactile data.

The above-mentioned reported studies have contributed greatly to the development of tactile codecs. However, there are two major shortcomings in these codecs that cannot be ignored in the real-time tactile applications of TI. The first main shortcoming is that these codecs are designed to compress either force-tactile data or vibrotactile data individually and cannot process both force-tactile data and vibrotactile data under a unified codec flowchart. For example, the transform-based vibrotactile codecs can efficiently process vibrotactile data, whereas it is difficult to efficiently process force-tactile data due to the low frequency of force-tactile signals. The other main shortcoming is that it is difficult for these codecs to trade off compression efficiency and codec delay. Specifically, the transform-based tactile codecs trade extra codec delay for better encoding performance. Once the codec delay exceeds the acceptable limits, the transform-based codecs struggle to satisfy the real-time requirements in TI applications. Although perception-based tactile codecs are less affected by codec delay, the quality of the decoded signals deteriorates drastically with increasing compression rate, resulting in their inability to synchronously stream and display multimedia interactive content in TI applications. As for the deep neural network model-based codecs, deep neural networks are costly to train, and the accuracy of the network has a significant impact on the performance of the codec.

Consequently, a versatile, real-time, and simple tactile codec with high compression efficiency and low codec delay for TI deserves further investigation. In this work, we are dedicated to developing a superior tactile codec for TI based on perceptual deadband and differential encoding, called TC-PDDE, which balances the reduction of packet size and the decrease of packet rate in tactile communication. Firstly, we adopt the perceptual deadband in the perceptual property to convert the original tactile signals into perceptible signals by discarding the imperceptible tactile signals. After that, we investigate a non-uniform quantizer according to the statistical properties of the perceptible tactile signals and adopt the entropy encoder to quantize and encode the differences of perceptible tactile signals. Finally, we validate the performance of the proposed TC-PDDE codec by comparing it with the

popular vibrotactile codecs and force-tactile codecs on the standard vibrotactile and self-built force-tactile datasets. In summary, the main contributions of this work are as follows.

- (1) We propose a versatile tactile codec for TI based on perceptual deadband and differential encoding, named TC-PDDE, which can process not only vibrotactile signals but also force-tactile signals under a unified codec flowchart.
- (2) We exploit the perceptual and statistical properties of tactile signals to achieve high-efficiency and low-delay compression by balancing the reduction of packet size and the decrease of packet rate in TC-PDDE.
- (3) We simulate a tele-ultrasound diagnosis scenario in the haptic tele-operation platform to establish a force-tactile dataset for validating the performance of TC-PDDE.
- (4) Our tactile codec TC-PDDE is the superior alternative for real-time tactile applications in TI. Comparison results on the standard vibrotactile dataset and self-built force-tactile dataset show TC-PDDE is a real-time tactile codec that provides superior compression efficiency and codec delay.

The rest of this article is organized as follows. Section 2 elaborates on the proposed tactile codec, including the preprocessing module, the differential compensation calculation module, an encoder, and a decoder. Section 3 details two datasets, a public vibrotactile dataset and a self-built force-tactile dataset, which are used to validate the performance of the different codecs. Comprehensive experiments under the vibrotactile and force-tactile datasets are proposed in Section 4. Finally, the work is concluded in Section 5.

2 The proposed tactile codec

In order to efficiently process vibrotactile and force-tactile signals under a unified codec flowchart and to improve the codec performance with respect to compression efficiency and codec delay, we propose a tactile codec based on the perceptual deadband and differential encoding, named TC-PDDE, using the perceptual and statistical properties of tactile signals for TI in this section.

2.1 The structure of TC-PDDE

The overall structure of TC-PDDE, as depicted in Figure 1, primarily comprises the preprocessing module, the differential compensation calculation module, an encoder module, a decoder module, and a reconstruction module. The preprocessing module converts the original tactile signals into perceptible signals based on the perceptual deadband. The differential compensation calculation module calculates the current differential compensations between the current perceptible signals and the previously transmitted signals. The encoder module encodes the differential compensations as the compressed signals into the binary bit stream. The decoder module decompresses the differential compensation bitstream. And the reconstruction module reconstructs the received differential compensations into the tactile signals according to the previous reconstruction signals.

When using the proposed TC-PDDE to process tactile signals, the processing flow, also as illustrated in Figure 1, can be divided into the encoding process and the decoding process. In the encoding process, the preprocessing procedure first utilizes the preprocessing module to convert the original tactile signals into perceptible signals. Next, the differential compensations procedure calculates the differential compensations between the current perceptible tactile signals and the previously transmitted signals. Subsequently, the normalization procedure normalizes the differential compensations to [-1,1], and a non-uniform quantization procedure quantizes differential compensations. Finally, an entropy encoder converts the differential compensations into a binary bitstream using the Huffman coding. As for the procedures in the decoding process of TC-PDDE, the binary bitstream is restored to the differential compensations through the entropy decoder, dequantizer, and inverse normalization. The reconstructed tactile signals are generated by the reconstruction module.

Detailed discussions of the procedures in the encoding and decoding processes of TC-PDDE are elaborated as follows.

(1) **Preprocessing:** The original tactile signals $\mathbf{S} = [S_1, S_2, \dots, S_{N-1}, S_N]$ are converted to perceptible tactile signals $\mathbf{s} = [s_1, \dots, s_i, \dots, s_n]$ $(N \ge n)$ according to the perceptual deadband, which can be expressed as

$$\begin{cases} k_i = \left| \frac{S_i - S_{i-1}}{S_{i-1}} \right| > k, \quad S_i \text{ transmits,} \\ k_i = \left| \frac{S_i - S_{i-1}}{S_{i-1}} \right| \leqslant k, \quad S_i \text{ remains,} \end{cases}$$

$$\tag{1}$$

where k is the Weber parameter in Webers Law, and the current newly generating signal S_i is transmitted only when the relative difference between the current signal and the previously transmitted signal S_{i-1} is larger than the just noticeable difference $k \cdot |S_{i-1}|$. What is noteworthy is that k is adjustable with stimulus [36].

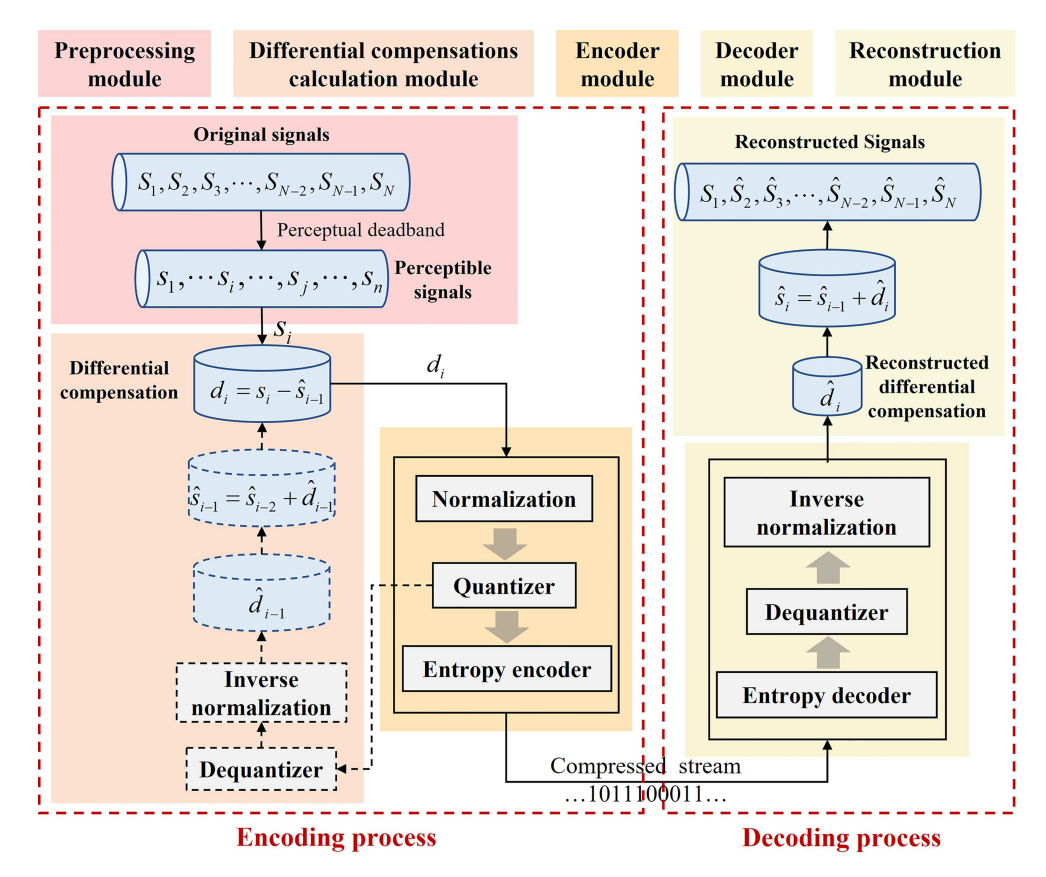


Figure 1 (Color online) The overall structure and processing flow of TC-PDDE.

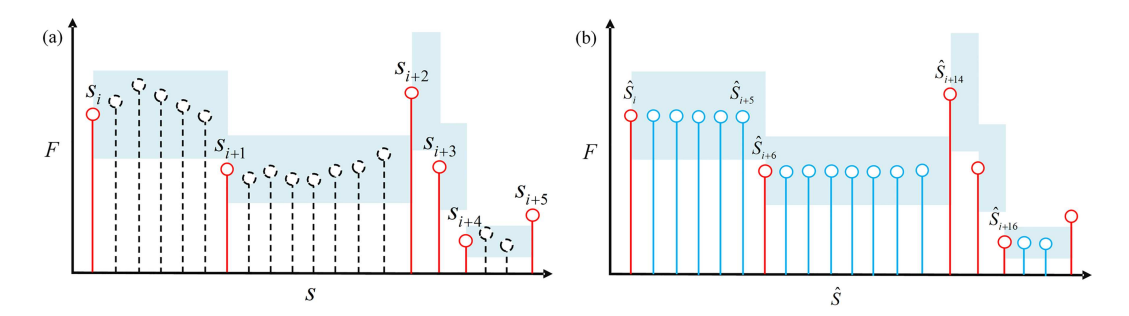


Figure 2 (Color online) Illustration of the (a) perceptual deadband and (b) reconstructed tactile signals.

As shown in Figure 2(a), red signals are perceptible signals, blue regions are the perceptual deadband of perceptible signals, and black dotted signals within the perceptual deadband are discarded signals. Apparently, the transmission of perceptible signals \mathbf{s} can decrease the packet rate of tactile signals to some extent compared to the transmission of the original signals \mathbf{S} .

(2) Differential compensation: Supposing that the previously transmitted perceptible tactile signal is s_{i-1} , the differential compensation d_i of current perceptible tactile signal s_i can be calculated by

$$d_i = s_i - s_{i-1}. \tag{2}$$

The variation interval $[d_{\min}, d_{\max}]$ of differential compensations $\mathbf{d} = [d_1, d_2, \dots, d_{n-2}, d_{n-1}]$ is much smaller than the counterpart $[s_{\min}, s_{\max}]$ of perceptible tactile signals \mathbf{s} when the sampling frequency is high, which requires fewer coding bits. Clearly, the transmission of differential compensations \mathbf{d} , rather than perceptible tactile signals \mathbf{s} , can decrease the packet size of tactile signals.

Given that lossless encoders are limited by Shannon's source coding theorem, we recommend the adoption of lossy encoders involving quantization. It implies that the decoded and reconstructed differential compensations $\hat{\mathbf{d}}$ may differ from the original differential compensations \mathbf{d} , resulting in errors \mathbf{e} between the reconstructed tactile

signals $\hat{\mathbf{s}}$ and the original perceptible tactile signal \mathbf{s} . To eliminate the error e_i , the differential compensation d_i should be calculated by

$$d_i = s_i - \hat{s}_{i-1},\tag{3}$$

where \hat{s}_{i-1} is the reconstructed tactile signal by the decoder. It should be noted that \hat{s}_{i-1} is reconstructed by the decoder at the transmitting end instead of the receiving end of the signal.

(3) Non-uniform quantization with varying digits: After calculating the differential compensations d, the quantizer is used to quantize d for reducing the coding bitrates. In TC-PDDE, a non-uniform quantizer with varying digits is utilized based on the statistical properties of differential compensations and the balance between the output bitstream and the quality of the recovered signals. The quantization procedure is listed as follows.

First, the polar code P_o , one digit, denotes the sign of the differential compensation d,

$$P_o = \begin{cases} 0, & \text{if } d < 0, \\ 1, & \text{otherwise,} \end{cases}$$
 (4)

where 0 and 1 indicate the positive and negative of d, respectively.

Second, the paragraph code P_c with varying digits is used to indicate the coarse range of |d|. Suppose |d| is quantized into 2^{10} levels and subsequently divided into 8 paragraphs including [0, 7], [8, 15], [16, 31], [32, 63], [64, 127], [128, 255], [256, 511], [512, 1023]-th levels, respectively. The paragraph indexes represented by binary with 3 digits are utilized to guide the coarse range of |d|:

$$K = \frac{|d|}{W_{\text{max}}} \cdot 2^{10},\tag{5}$$

$$P_{c} = \begin{cases} 000, & \text{when } \log_{2}K < 3, \\ \text{BIN}\left(\lfloor \log_{2}K - 2 \rfloor\right), & \text{when } 3 \leq \log_{2}K \leq 10, \\ 111, & \text{when } \log_{2}K > 10, \end{cases}$$
 (6)

where BIN(·) means translating a decimal integer into binary code and notation $\lfloor \cdot \rfloor$ stands for rounding down; W_{max} is the maximum quantization weight to ensure that the values of K are smaller than 2^{10} .

From (5) and (6), it can be deduced that a larger maximum quantization weight W_{max} leads to more concentrated P_c , and W_{max} can adjust the number of paragraph index digits. When the value of W_{max} is greater than 64, the value of K in (5) is less than 16, which means that only the first two paragraphs [0, 7] and [8, 15] are active and the others are inactive. Therefore, 1 digit is competent to represent the paragraph indexes, and Eq. (6) is transformed into

$$P_c = \begin{cases} 0, & \text{when } \log_2 K < 3, \\ 1, & \text{when } \log_2 K \geqslant 3. \end{cases}$$
 (7)

Moreover, when the value of W_{max} is greater than 16, the value of K in (5) is less than 64, then the first four paragraphs [0,7], [8,15], [16,31] and [32,63] are active and the others are inactive. Hence, the paragraph indexes should be represented by 2 digits, and Eq. (6) can be rewritten as

$$P_c = \begin{cases} 00, & \text{when } \log_2 K < 3, \\ \text{BIN}\left(\lfloor \log_2 K - 2 \rfloor\right), & \text{when } 3 \leqslant \log_2 K \leqslant 6, \\ 11, & \text{when } \log_2 K > 6. \end{cases}$$

$$(8)$$

Third, the paragraph inner code I_c means the fine range of |d| within the specific paragraph. Every paragraph is split into 8 smaller segments, and the indices of these sub-segments are used to recognize the precise range of |d|. Assuming that the value of K corresponding to the differential compensation d_i is K_i , and $K_i \in [L_K, U_K]$, then the sub-segment indexes represented by binary, i.e., the paragraph inner code I_c , can be obtained by

$$I_c = \begin{cases} \text{BIN}\left(\left\lfloor \frac{K_i - L_K}{U_K - L_K} \cdot 2^3 \right\rfloor\right), & \text{if } K_i < U_K, \\ 111, & \text{otherwise.} \end{cases}$$
(9)

To illustrate the above quantization procedure more clearly, a brief example is presented. Let the differential compensation $d_i = 0.5$ and the quantization weight $W_{\text{max}} = 10$, the polar code P_o of d_i is 1 since $d_i > 0$. Next, $K_i = 51.2$ leads to the paragraph code $P_c = \text{BIN}(3) = 011$. After that, due to $K_i \in [32, 63]$, $L_K = 32$ and $U_K = 63$,

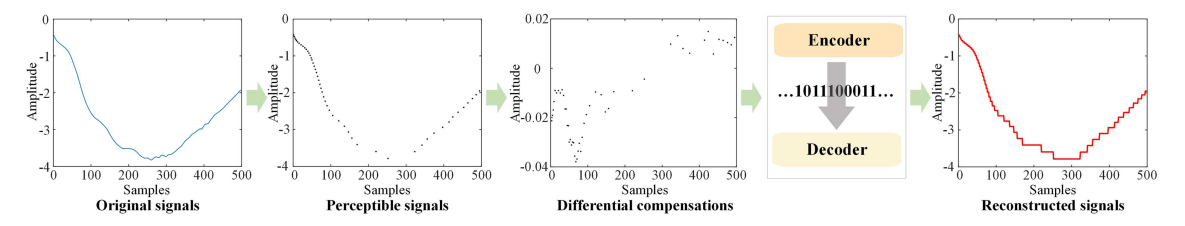


Figure 3 (Color online) The input and output signals of different modules in TC-PDDE.

the paragraph inner code $I_c = \text{BIN}(4) = 100$. As a result, the quantized code of the differential compensation $d_i = 0.5$ is 1011100 when $W_{\text{max}} = 10$. Moreover, the quantized code of $d_i = 0.5$ is 101010 when $W_{\text{max}} = 50$ and the quantized code of $d_i = 0.5$ is 10101 when $W_{\text{max}} = 100$. It is obvious that digits of the quantized code for the differential compensation d are not fixed but vary according to the quantization weight W_{max} , which can adaptively reduce the coding bitrates.

- (4) Huffman encoder: At last, the entropy encoder is deployed to encode quantized differential compensations \mathbf{d} to achieve a greater reduction of stream bitrates without any loss. The statistical result reveals that different quantized codes appear with different frequencies under the effect of the maximum quantization weight W_{max} . Therefore, we use the popular Huffman encoder, in which the frequently occurring fixed-length sequences are mapped to shorter binary sequences, to compress the quantized codes.
- (5) The decoder: The decoder in TC-PDDE mainly contains the entropy decoder, dequantizer, and inverse normalization. At the beginning of the decoding process in TC-PDDE, the Huffman decoder recomposes the quantized differential compensations from the bit stream in accordance with the inverse mapping. Afterward, the dequantizer restores the differential compensations from the quantized codes, which include polar codes, paragraph codes, and segment inner codes. Subsequently, the reconstructed differential compensation \hat{d}_i is generated by the inverse normalization. Finally, the reconstructed perceptible tactile signal \hat{s}_i can be formulated by

$$\hat{s}_i = \hat{s}_{i-1} + \hat{d}_i. \tag{10}$$

Furthermore, the reconstructed tactile signals \hat{S} are depicted in Figure 2(b), in which the red reconstructed signal \hat{S}_i is the reconstructed perceptible tactile signal \hat{s}_i , and the blue signals in the perceptual deadband are reconstructed using the zero-order hold method. In the zero-order hold method, if the receiving end receives a signal at time node t_i and does not receive a signal at time node t_{i+1} , then the signal at t_{i+1} is held the same as the signal at t_i . Thus, $\hat{S}_{i+1} = \cdots = \hat{S}_{i+5} = \hat{S}_i = \hat{s}_i$ and $\hat{S}_{i+7} = \cdots = \hat{S}_{i+13} = \hat{S}_{i+6} = \hat{s}_{i+1}$ in Figure 2(b).

2.2 The feature of TC-PDDE

To intuitively demonstrate the feature of TC-PDDE, an illustration of the input and output signals of all modules in TC-PDDE is shown in Figure 3. Combined with Figure 3 and the above description of the structure of TC-PDDE, it can be observed that the original tactile signals are first converted to perceptible signals by the perceptual deadband in the preprocessing module; after that, perceptible signals are transformed into differential compensations in the differential compensation calculation module; subsequently, the differential compensations are encoded into the binary bit stream by non-uniform quantization with varying digits and Huffman decoder in the encoder module; finally, the bitstream is recovered into differential compensations in the decoder module, and the recovered differential compensations are further reconstructed into perceptible signals with acceptable information loss in the reconstruction module.

According to the above description of the tactile signals transformation process in TC-PDDE, it can be analyzed that TC-PDDE is characterized by the combination of perceptual deadband and differential encoding. The perceptual deadband is employed in the preprocessing module to reduce the packet rate of tactile signals and maintain the distortion of reconstructed signals under the human perceptual threshold by discarding redundant tactile signals within the perceptual deadband and transmitting only the tactile signals beyond the perceptual deadband. At the same time, the differential encoding comprising the differential compensation calculation module and encoder module can decrease the packet size of tactile signals, due to the variation interval of differential compensations between two adjacent perceptible tactile signals being much smaller than the variation interval of the perceptible tactile signals, requiring fewer coding bits. Overall, TC-PDDE endeavors to simultaneously reduce the packet rate and decrease the packet size of tactile signals, enhancing the coding performance of the tactile codec.

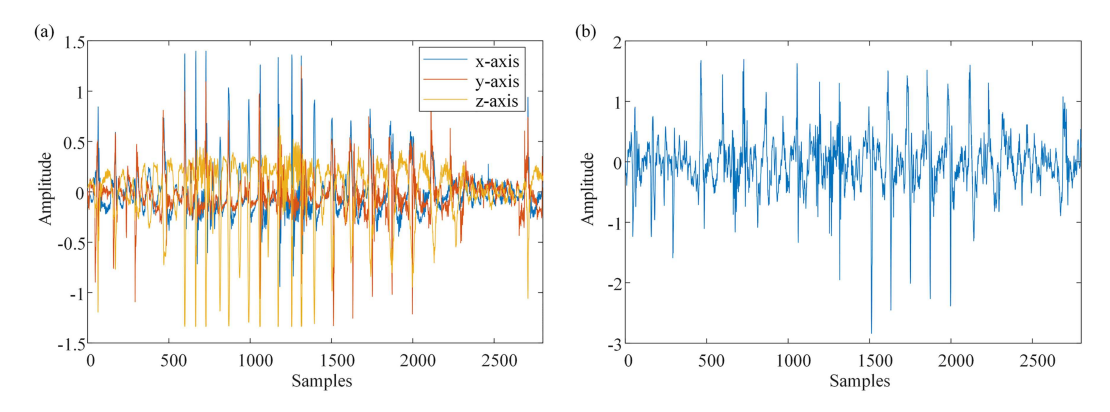


Figure 4 (Color online) The partial vibrotactile signals in the public vibrotactile dataset. (a) The original three-dimensional vibrotactile signals; (b) the converted one-dimensional vibrotactile signals.

3 Vibrotactile and force-tactile datasets

In this section, we introduce two tactile datasets, a public vibrotactile dataset and a self-built force-tactile dataset, to illustrate the properties of vibrotactile signals and force-tactile signals. More importantly, these two tactile datasets will be used to validate the performance of TC-PDDE in the next section.

3.1 The public vibrotactile dataset

In order to facilitate a fair comparison of the performance of different vibrotactile codecs by researchers, the IEEE P1918.1.1 group has established a public standard dataset [37] that contains vibrotactile signals for nine materials at different exploration speeds. There are a total of 280 vibrotactile data traces in this dataset, and each trace consists of 3360–8400 samples with each sample represented by a 16-bit pulse code. All 3-dimensional vibrotactile signals are converted into 1-dimensional signals using the DFT321 algorithm [38] according to the proposal of the IEEE P1918.1.1 group. Since the sampling rate is set to 2.8 kHz, the raw bit rate of this public dataset is 44.8 kbps.

Moreover, the partial vibrotactile signals in the dataset are illustrated in Figure 4. Combining Figure 4 and the analysis of the standard vibrotactile dataset, it can be noticed that the vibrotactile signals have three statistical characteristics, including low amplitude, high sampling rate, and high sensitivity [34], which increases the challenge of achieving efficient data compression without compromising signal quality.

3.2 The self-built force-tactile dataset

To establish a force-tactile dataset, we simulate a tele-ultrasound diagnostic scenario on the haptic tele-operation platform (HapTop) [39]. As shown in Figure 5, the HapTop platform consists mainly of three domains, the master domain, the network domain, and the slave domain. In the master domain, the commercial six-dimensional haptic device Geomagic Touch is employed as a controller to remotely manipulate the actuator in the slave domain by control commands and as a tactile actuator to present tactile signals sent from the slave domain. In the slave domain, the robotic arm UR3 is utilized as the actuator to accurately replicate the actions of the user according to the control commands sent from the master domain, and the ultrasonic probe and the force/torque sensor ATI Nano 17 with digital I/O device NI USB-6210 are used to capture force-tactile information and ultrasound image information during interaction with the remote environment. And the network domain is the communication bridge between the master and slave domains. We implement communication between two domains over the Internet, utilizing sockets for data transmission.

Based on the HapTop platform described above, we simulate a tele-ultrasound diagnostic scenario to acquire the force-tactile dataset. In this scenario, the user manipulates the controller Geomagic Touch in the master domain to generate control commands, which are sent to the slave domain through the network domain. The UR3 in the slave domain replicates the actions of the user and scans the experimental dummy according to the control commands, while the ATI Nano 17 acquires the force-tactile data in real-time as the ultrasonic probe interacts with the experimental dummy. We collect a total of 10 sets of tactile signals with the ATI Nano17 at a fixed sampling rate of 1.0 kHz, and the 16-digit pulse-code is used to represent the force-tactile data, yielding a raw bitrate of 48 kbps.

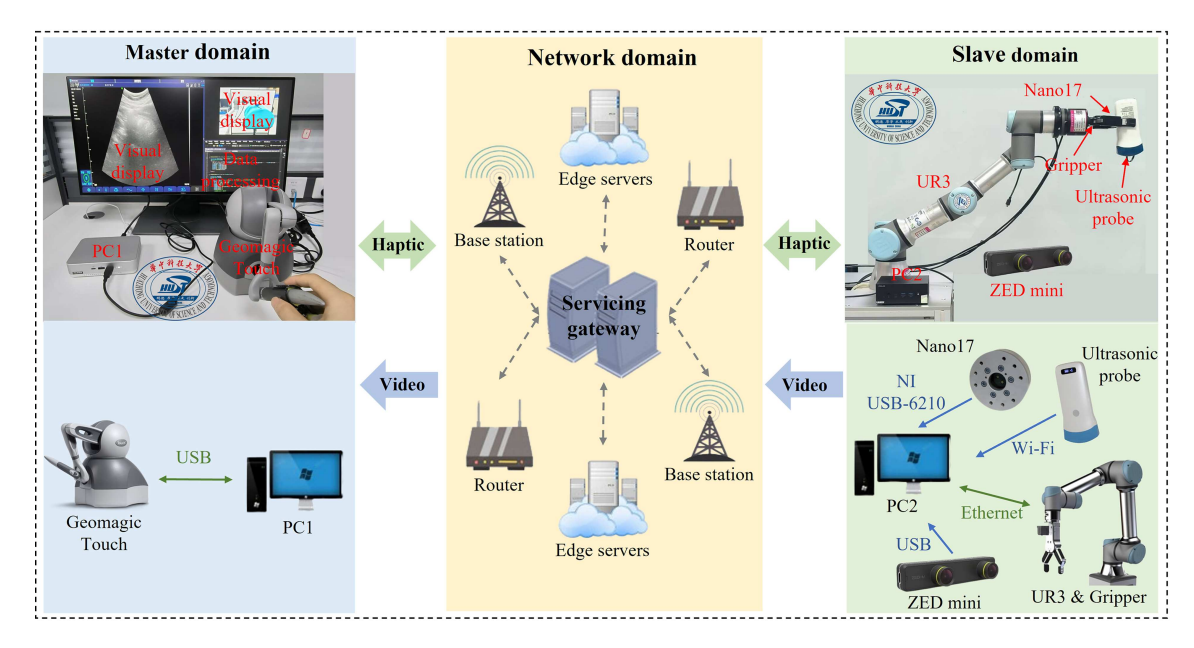


Figure 5 (Color online) The hardware configuration and data flow of the HapTop platform in a tele-ultrasound diagnostic scenario.

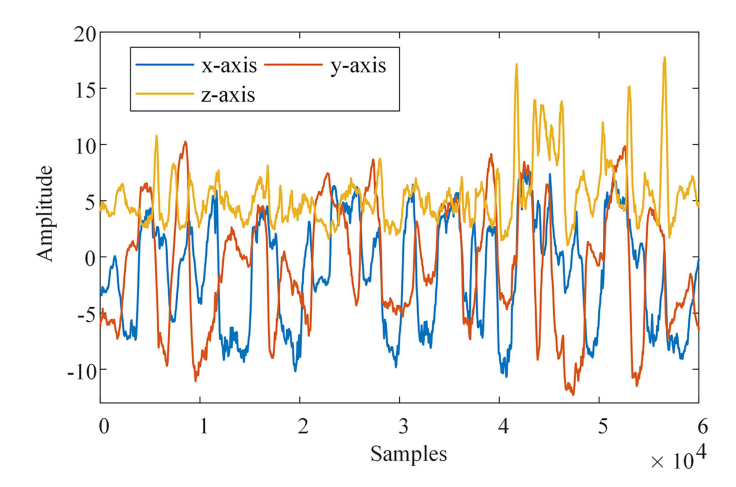


Figure 6 (Color online) The partial force-tactile signals in the simulated tele-ultrasound diagnostic scenario.

Furthermore, the partial force-tactile signals in the dataset are depicted in Figure 6. Different from vibrotactile signals, force-tactile signals have a wider amplitude fluctuation interval and a lower sampling rate, resulting in lower sensitivities, which means that force-tactile signals can achieve higher compression efficiency while retaining high quality.

4 Experiment and discussion

In this section, we validate the performance of the proposed TC-PDDE with respect to compression efficiency and codec delay. First, we introduce four metrics to quantitatively evaluate the codecs. Second, we demonstrate the superiority of TC-PDDE by comparing it with existing vibrotactile codecs, such as RNVC [34], VPC-DS [30], PVC-SLP [29], and VC-PWQ [31], on the public vibrotactile dataset. Third, we present the advantages of TC-PDDE with comparisons to existing force-tactile codecs, such as the PD-based [18] and DCT-based [22] codecs, on the self-built force-tactile dataset. Finally, we compare the codec delay of all the above codecs. It should be stated that we implement and validate our codec with MATLAB R2023b in an Intel[®] Core(TM) i9-13900HX CPU@4.80 GHz PC.

4.1 The metrics to evaluate compression efficiency

To evaluate the compression efficiency of various tactile codecs quantitatively, four metrics containing the compression ratio (CR), which indicates the compression effectiveness, the signal-to-noise ratio (SNR) and the peak signal-to-noise ratio (PSNR), which means the objective quality of the reconstruction signals, and the spectral temporal similarity (ST-SIM) [40], which reflects the similarity of tactile signals, are introduced.

The CR metric represents the ratio of original bitrates to compressed bitrates, which can be formulated as

$$CR = \frac{\text{original_bitrate}}{\text{compressed_bitrate}},$$
(11)

where the original_bitrate can be calculated by $f_s \cdot L$, f_s is the sample frequency, and L is the coded bits of every sample. For example, if a signal acquired at the sample frequency $f_s = 1$ kHz is coded with L = 16 bits/sample, the original bitrate is 16.0 kbps.

The SNR metric is calculated as a logarithmic ratio between the powers of the original signal and the reconstruction error,

$$SNR = 10 \cdot \log_{10} \left(\frac{\sum_{n \in N} \|S_n\|^2}{\sum_{n \in N} \|S_n - \hat{S}_n\|^2} \right), \tag{12}$$

where \hat{S}_n and S_n are the reconstructed tactile signals and original tactile signals, respectively, and N is the total amount of data in the original signal.

The PSNR metric can be formulated as

$$PSNR = 10 \cdot \log_{10} \left(\frac{\|S_{\text{max}} - S_{\text{min}}\|^2}{\text{MSE}} \right), \text{ where MSE} = \frac{1}{N} \sum_{n \in N} \left\| S_n - \hat{S}_n \right\|^2,$$
 (13)

where S_{max} and S_{min} are the maximum and minimum values of the original force-tactile signals \mathbf{S} , MSE denotes the mean square function of the reconstructed force-tactile signals $\hat{\mathbf{S}}$ and original force-tactile signals \mathbf{S} .

The ST-SIM metric serves as a comprehensive objective quality measure for tactile signal similarity, incorporating a spatial indicator and a temporal indicator. The expression of ST-SIM is formulated as

$$ST-SIM = \left(\frac{1}{N_s} \sum_{k_s=1}^{N_s} S-SIM_{k_s}\right)^{\eta} \cdot \left(\frac{1}{N_s} \sum_{k_s=1}^{N_s} T-SIM_{k_s}\right)^{(1-\eta)}, \tag{14}$$

where $\eta \in [0, 1]$ is a weighting factor to emphasize the importance of S-SIM and T-SIM, N_s means the count of segments used to compute S-SIM and T-SIM. ST-SIM is briefly described here since the calculation expressions of S-SIM and T-SIM are tedious, and more details can be referred to [40].

4.2 The compression efficiency of TC-PDDE on vibrotactile dataset

When processing tactile signals using the proposed tactile codec TC-PDDE, the Weber parameter k in the reprocessing module and the maximum quantization weight W_{max} in the encoder module have a significant impact on the performance of TC-PDDE. Thus, we jointly adjust k and W_{max} to reveal the relationships between CR, SNR, PSNR, and ST-SIM in TC-PDDE. First, we set k to a series of sequences between [0,1], and calculate the corresponding values of CR, SNR, PSNR, and ST-SIM by adjusting W_{max} in the range of [1,100] for every value of k. Then, we identify the optimal combination of k and W_{max} that yields a better encoder performance according to the variation trends of SNR vs. CR. Finally, we calculate PSNR and ST-SIM with the identified parameters and obtain the variation trends of PSNR vs. CR and ST-SIM vs. CR.

Following the procedures outlined above, we validate the performance of the proposed tactile codec TC-PDDE on the public vibrotactile dataset. The fitted variation trends of SNR vs. CR, PSNR vs. CR, and ST-SIM vs. CR of TC-PDDE are illustrated in Figure 7. Obviously, by adjusting the Weber parameter k and maximum quantization weight W_{max} , TC-PDDE can achieve a wide range of CRs while maintaining the high perceptual quality (SNR, PSNR, or ST-SIM) of the reconstructed signals. More specifically, when the CR of TC-PDDE reaches 40, the SNR, PSNR, or ST-SIM still remain at 5.02 dB, 46.20 dB, and 0.88, respectively.

At the same time, we compare the proposed tactile codec TC-PDDE with popular vibrotactile codecs, such as RNVC, VPC-DS, PVC-SLP, and VC-PWQ, with respect to SNR, PSNR, and ST-SIM on the public vibrotactile dataset, the comparison results are also presented in Figure 7. It can be found from Figure 7 that TC-PDDE

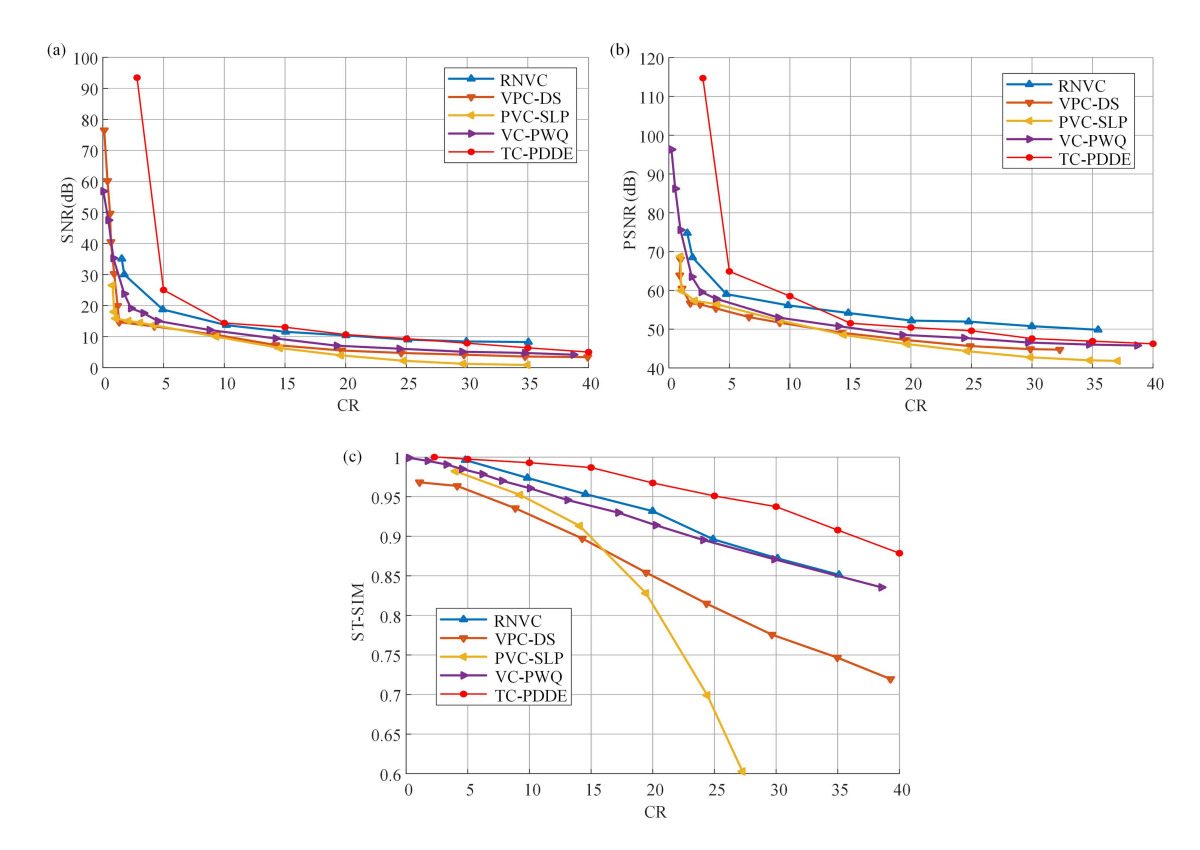


Figure 7 (Color online) The quality-CR curves for comparison on the vibrotactile dataset. (a) CR vs. SNR; (b) CR vs. PSNR; (c) CR vs. ST-SIM.

can obtain superior SNRs, PSNRs, and ST-SIMs at the same CRs, or alternatively, superior CRs at the same SNRs, PSNRs, and ST-SIMs, in comparison with VPC-DS, PVC-SLP, and VC-PWQ. RNVC can be comparable to TC-PDDE concerning SNR and PSNR; however, CR and ST-SIM of RNVC are inferior to the counterparts of TC-PDDE, which suggests that the vibrotactile signals reconstructed by TC-PDDE have higher perceptibility. As a result, our tactile codec provides more superiority than the popular vibrotactile codecs in terms of compression efficiency on the public vibrotactile dataset.

Additionally, to visually display the outcome of the proposed TC-PDDE, Figure 8 shows the comparisons between the partial original and reconstructed vibrotactile signals with CR of 5, 20, and 40. It can be seen that TC-PDDE can reconstruct vibrotactile signals without a significant loss in perceptual quality even at a compression rate of 40, which intuitively verifies the superior performance of TC-PDDE.

4.3 The compression efficiency of TC-PDDE on force-tactile dataset

As with the processing of the vibrotactile dataset, we adopt the force-tactile signals on the x-axis in the self-built force-tactile dataset to evaluate the performance of the proposed tactile codec TC-PDDE. The fitted SNR vs. CR, PSNR vs. CR, and ST-SIM vs. CR curves of TC-PDDE are plotted in Figure 9. It can be observed from Figure 9 that TC-PDDE can compress the force-tactile signals over a wide range of CR while preserving the high perceptual quality (SNR, PSNR, or ST-SIM) of the reconstructed signals by adjusting the Weber parameter k and maximum quantization weight W_{max} . In particular, the CR of TC-PDDE can reach 160, and the SNR, PSNR, and ST-SIM can still be maintained at 29.84 dB, 48.41 dB, and 0.80, respectively.

Meanwhile, TC-PDDE is also compared with the widely used force-tactile data compression algorithms including PD-based and DCT-based codecs with SNR vs. CR, PSNR vs. CR, and ST-SIM vs. CR curves on the self-built force-tactile dataset, and the comparison results are also presented in Figure 9. Apparently, the CR of the TC-PDDE is much wider than the PD-based and DCT-based codecs, and the larger the CR, the better the performance of TC-PDDE is against the PD-based and DCT-based codecs.

Furthermore, in order to visualize the codec results of the proposed TC-PDDE, Figure 10 displays the comparison between the partial original force-tactile signals and the reconstructed force-tactile signals when the CR values are 10, 30, 60, 90, 120, and 150. It can be observed that the proposed TC-PDDE is able to reconstruct the force-

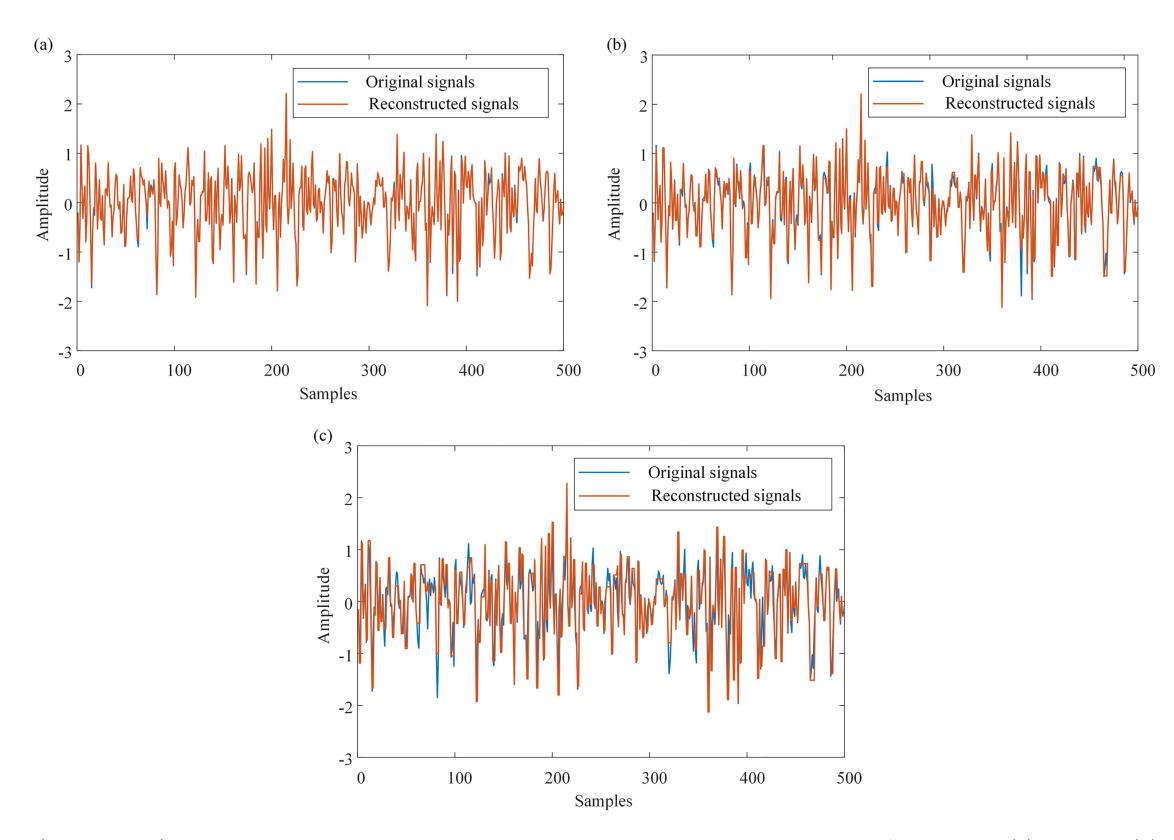


Figure 8 (Color online) The comparisons of the original and reconstructed vibrotactile signals at different CRs. (a) CR = 5; (b) CR = 20; (c) CR = 40.

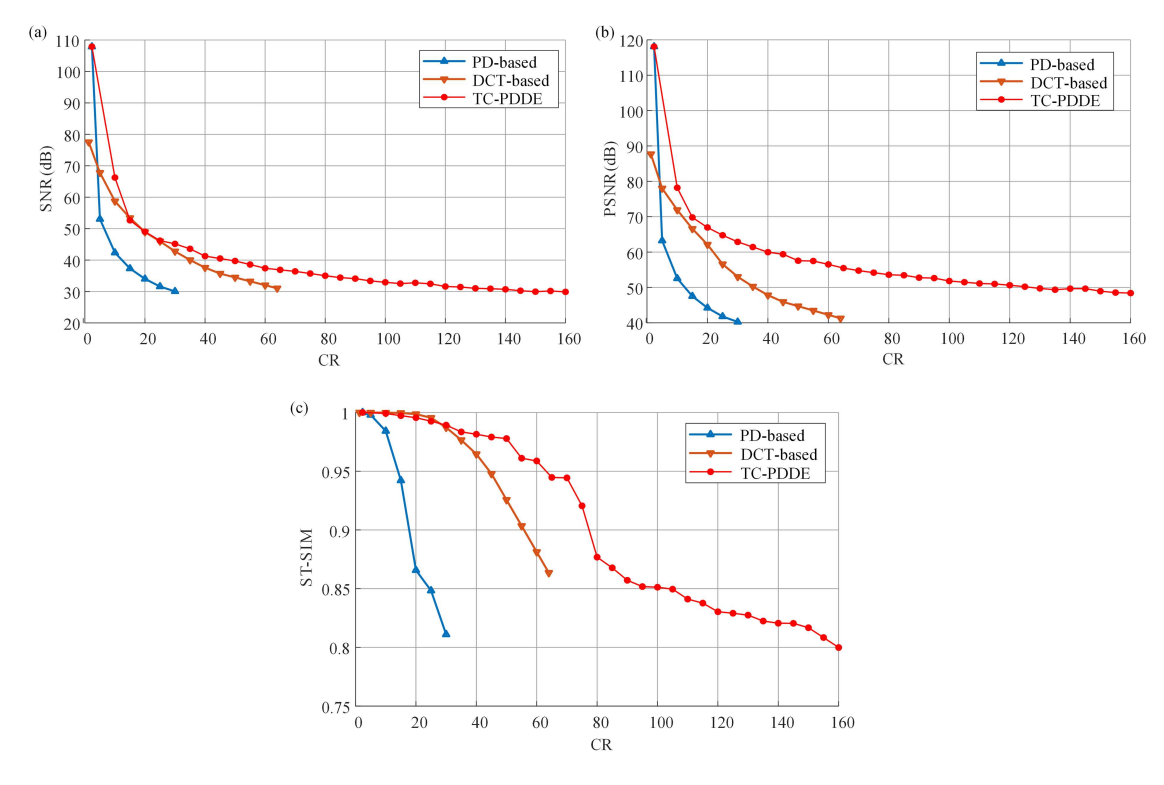


Figure 9 (Color online) The quality-CR curves for comparison on the force-tactile dataset. (a) CR vs. SNR; (b) CR vs. PSNR; (c) CR vs. ST-SIM.

tactile signals without a significant loss of perceptual quality even at a compression rate of 150, providing intuitive

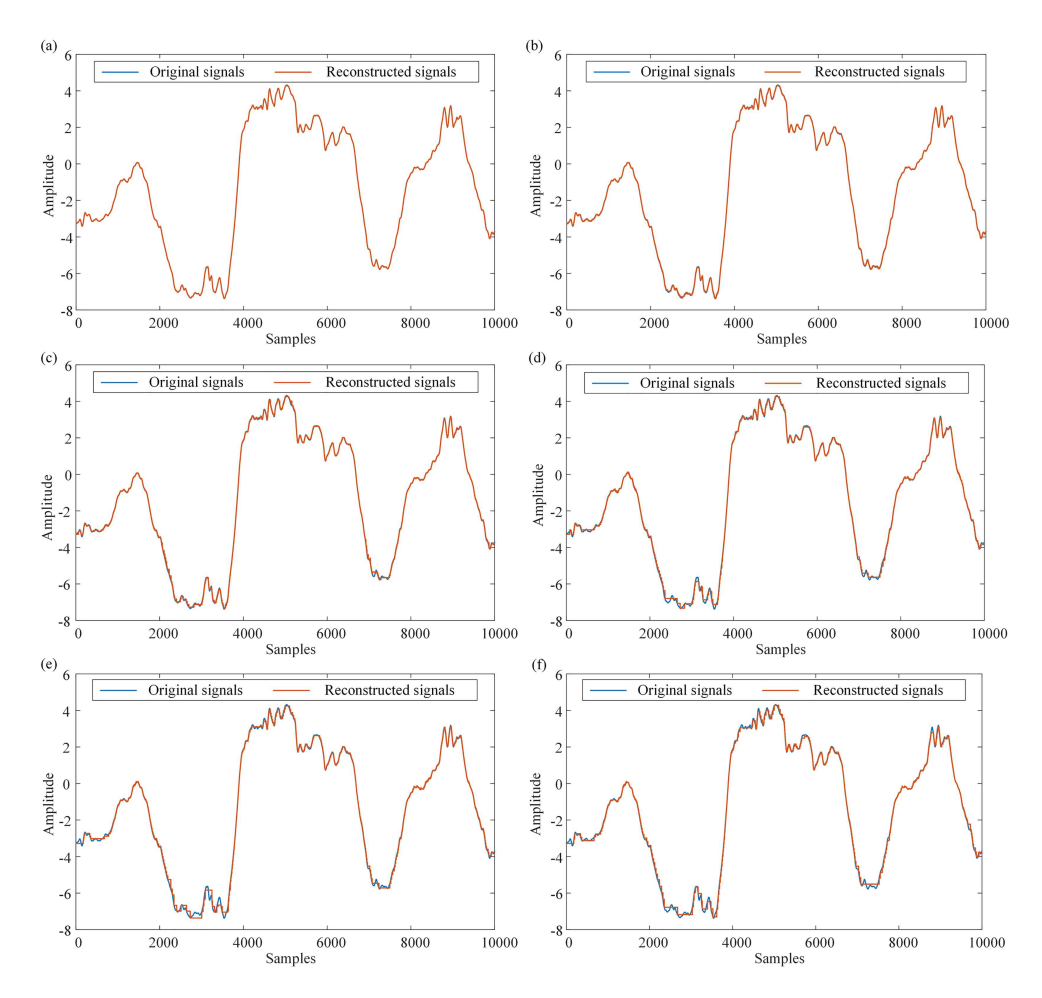


Figure 10 (Color online) The comparisons of the original and reconstructed vibrotactile signals at different CRs. (a) CR = 10; (b) CR = 30; (c) CR = 60; (d) CR = 90; (e) CR = 120; (f) CR = 150.

verification of the excellent performance of TC-PDDE.

4.4 The codec delay of TC-PDDE

In addition to the compression efficiency, we also compared the codec delay of the codecs mentioned above. The codec delay mainly includes the average encoding delay, buffer delay (time to collect sufficient samples for simultaneous processing), and average decoding delay. The comparison results are listed in Table 1. The average encoding delay and the average decoding delay of RNVC, VPC-DS, and PVC-SLP are extracted from [29,30,34]; the average encoding delay and average decoding delay of PD, DCT, and TC-PDDE are acquired through our experiments. The average encoding delay and average decoding delay of the proposed tactile codec TC-PDDE are 0.42 and 0.41 ms, respectively. TC-PDDE outperforms other codecs, except for the PD-based force-tactile codec, in terms of average coding delay and average coding delay owing to factors such as the sample-by-sample processing mechanism and the simple but efficient codec flowchart.

Moreover, the buffer delays of the above-mentioned codecs are also recorded in Table 1. RNVC introduces a NULL flag to represent the number of successive repetitions of a sample, and the maximum number of successive repetitions is 32 in RNVC. Since the sampling rate of the standard vibrotactile dataset is 2.8 kHz, the maximum buffer delay of RNVC is 11.4 ms. Similarly, the block length of 512 samples is used to validate the codec performance in VPC-DS and VC-PWQ, and the frame length of 200 samples is utilized to validate the codec performance in PVC-SLP. Thus, the buffer delays of VPC-DS and VC-PWQ are 182.9 ms, and the buffer delay of PVC-SLP is 71.4 ms. In DCT, 128 samples are set into one block for compression; the buffer delay of DCT is 128 ms due to the sampling rate of the force-tactile dataset being 1 kHz. Different from the above codecs, the proposed tactile codec TC-PDDE is the real-time codec with 0 buffer delay since it can process the data sample-by-sample, instead of buffering data. Considering that the human threshold for the perception of tactile delay is 40 ms [41] in real-time applications, TC-PDDE is not only applicable to real-time applications in TI but also provides more delay

Table 1 Comparisons of delays in different codecs.

	RNVC	VPC-DS	PVC-SLP	VC-PWQ	PD	DCT	TC-PDDE
Encoding delay (ms)	1	4.3 - 26.3	20.5	_	0.06	1.26	0.42
Decoding delay (ms)	0.6	_	8.2	_	0.04	0.68	0.41
Buffer delay (ms)	0-11.4	182.9	71.4	182.9	0	128	0

redundancy for long-distance tactile communication.

5 Conclusion

To develop a versatile, real-time, and simple tactile codec with higher compression efficiency and lower codec delay for TI, this work presents a tactile codec based on perceptual deadband and differential encoding, called TC-PDDE, by simultaneously reducing the packet size and decreasing the packet rate of tactile signals. We suggest an encoder including tactile data preprocessing on the basis of the perceptual deadband, differential calculation, non-uniform quantization of differential compensations and an entropy encoder, and decoders corresponding to the encoder modules. Aiming to validate the performance of TC-PDDE, we simulate a tele-ultrasound diagnosis scenario in the haptic tele-operation platform to establish a force-tactile dataset and compare TC-PDDE with existing vibrotactile and force-tactile codecs on the standard vibrotactile dataset and the self-built force-tactile dataset. The comparison results demonstrate that TC-PDDE not only achieves higher compression efficiency but also lower codec delay, indicating that TC-PDDE is the superior alternative for real-time tactile applications in TI.

However, the proposed TC-PDDE codec can only process vibrotactile or force-tactile signals individually, and can be considered a unimodal tactile codec. In complex real-world scenarios, such as a tactile tele-operation scenario, where multiple tactile modalities work together to provide tactile feedback, coding and decoding multimodal tactile signals are necessary for efficient transmission of signals. Therefore, how to develop multimodal tactile codecs is our future research work.

References

- 1 Fettweis G P. The Tactile Internet: applications and challenges. IEEE Veh Technol Mag, 2014, 9: 64-70
- 2 Chen Y, Li A, Wu D, et al. Toward general cross-modal signal reconstruction for robotic teleoperation. IEEE Trans Multimedia, 2024, 26: 3541–3553
- 3 Chen Y, Li P, Li A, et al. Toward low-latency cross-modal communication: a flexible prediction scheme. IEEE Trans Mobile Comput, 2024, 23: 13310–13324
- 4 Mumtaz S, Bo A, Al-Dulaimi A, et al. Guest editorial 5G Tactile Internet: an application for industrial automation. IEEE Trans Ind Inform, 2019, 15: 2992–2994
- 5 Liu G, Wang H, Wang C, et al. Federated double deep Q-networks for unbalanced material classification in Tactile Internet. IEEE Trans Ind Inf, 2024, 20: 14351–14360
- 6 Wei X, Duan Q, Zhou L. A QoE-driven Tactile Internet architecture for smart city. IEEE Netw, 2020, 34: 130–136
- 7 Liu H, Deng Y, Guo D, et al. An interactive perception method for warehouse automation in smart cities. IEEE Trans Ind Inf, 2021, 17: 830–838
- 8 Kusuma H M, Shukla V K, Gupta S. Enabling VR/AR and tactile through 5G network. In: Proceedings of 2021 International Conference on Communication Information and Computing Technology (ICCICT), 2021. 1–6
- 9 Li A, Chen Y, Ni S, et al. Haptic signal reconstruction in eHealth Internet of Things. IEEE Internet Things J, 2022, 9: 17047–17057
- 10 Shi W, Yao J C, Xu J D, et al. Empowering over-the-air personalized federated learning via RIS. Sci China Inf Sci, 2024, 67: 219302
- 11 Shi W, Xu J, Xu W, et al. On secrecy performance of RIS-assisted MISO systems over Rician channels with spatially random eavesdroppers. IEEE Trans Wireless Commun, 2024, 23: 8357–8371
- 12 Steinbach E, Strese M, Eid M, et al. Haptic codecs for the Tactile Internet. Proc IEEE, 2019, 107: 447–470
- 13 Emami M, Bayat A, Tafazolli R, et al. A survey on haptics: communication, sensing and feedback. IEEE Commun Surv Tutorials, 2025, 27: 2006–2050
- 14 Li Q, Kroemer O, Su Z, et al. A review of tactile information: perception and action through touch. IEEE Trans Robot, 2020, 36: 1619–1634
- 15 Gao Y, Wu D, Zhou L. How to improve immersive experience? IEEE Trans Multimedia, 2024, 26: 8691-8703
- Hinterseer P, Steinbach E, Hirche S, et al. A novel, psychophysically motivated transmission approach for haptic data streams in telepresence and teleaction systems. In: Proceedings of IEEE International Conference on Acoustics, Speech, and Signal Processing, 2005. 1097-1100
- 17 Hinterseer P, Hirche S, Chaudhuri S, et al. Perception-based data reduction and transmission of haptic data in telepresence and teleaction systems. IEEE Trans Signal Process, 2008, 56: 588–597
- 18 Bhardwaj A, Cizmeci B, Steinbach E, et al. A candidate hardware and software reference setup for kinesthetic codec standardization. In: Proceedings of IEEE International Symposium on Haptic, Audio and Visual Environments and Games (HAVE), 2017. 1–6
- 19 Xu Y, Huang Q, Zheng Q, et al. Perception-based prediction for efficient kinesthetic coding. IEEE Signal Process Lett, 2024, 31: 2530–2534
- 20 Liu X, Dohler M. A data-driven approach to vibrotactile data compression. In: Proceedings of IEEE International Workshop on Signal Processing Systems (SiPS), 2019. 341–346
- 21 Chaudhari R, Schuwerk C, Danaei M, et al. Perceptual and bitrate-scalable coding of haptic surface texture signals. IEEE J Sel Top Signal Process, 2015, 9: 462–473
- 22 Tanaka H, Ohnishi K. Haptic data compression/decompression using DCT for motion copy system. In: Proceedings of IEEE International Conference on Mechatronics, 2009. 1–6
- 23 Tanaka H, Ohnishi K. Lossy data compression using FDCT for haptic communication. In: Proceedings of 11th IEEE International Workshop on Advanced Motion Control (AMC), 2010. 756–761

- 24 Okamoto S, Yamada Y. Perceptual properties of vibrotactile material texture: effects of amplitude changes and stimuli beneath detection thresholds. In: Proceedings of IEEE/SICE International Symposium on System Integration, 2010. 384–389
- 25 Kuzu A, Baran E A, Bogosyan S, et al. Wavelet packet transform-based compression for teleoperation. J Syst Control Eng, 2015, 229: 639–651
- 26 Baran E A, Kuzu A, Bogosyan S, et al. Comparative analysis of a selected DCT-based compression scheme for haptic data transmission. IEEE Trans Ind Inf, 2016, 12: 1146–1155
- 27 Zeng C Y, Zhao T C, Liu Q, et al. Perception-lossless codec of haptic data with low delay. In: Proceedings of 28th ACM International Conference on Multimedia, 2020. 3642–3650
- 28 Hassen R, Steinbach E. Vibrotactile signal compression based on sparse linear prediction and human tactile sensitivity function. In: Proceedings of IEEE World Haptics Conference (WHC), 2019. 301–306
- 29 Hassen R, Gulecyuz B, Steinbach E. PVC-SLP: perceptual vibrotactile-signal compression based-on sparse linear prediction. IEEE Trans Multimedia, 2021, 23: 4455–4468
- 30 Noll A, Gülecyüz B, Hofmann A, et al. A rate-scalable perceptual wavelet-based vibrotactile codec. In: Proceedings of IEEE Haptics Symposium (HAPTICS), 2020. 854–859
- 31 Noll A, Nockenberg L, Gülecyüz B, et al. VC-PWQ: vibrotactile signal compression based on perceptual wavelet quantization. In: Proceedings of IEEE World Haptics Conference (WHC), 2021. 427–432
- 32 Liu G, Li X, Wang C, et al. Online compression and reconstruction for communication of force-tactile signals. IEEE Commun Lett, 2023, 27: 981–985
- 33 Deng Q, Mahmoodi T, Aghvami A H. A long short-term memory-based model for kinesthetic data reduction. IEEE Internet Things J, 2023. 10: 16975-16988
- 34 Zhao T, Fang Y, Wang K, et al. High efficiency vibrotactile codec based on gate recurrent network. IEEE Trans Multimedia, 2023, 25: 5043–5052
- 35 Xu Y, Chen D, Fang Y, et al. Efficient vibrotactile codec based on Nbeats network. IEEE Signal Process Lett, 2024, 31: 2845-2849
- 36 Hirche S, Buss M. Human-oriented control for haptic teleoperation. Proc IEEE, 2012, 100: 623-647
- 37 Kirsch J, Strese M, Liu Q, et al. A low-cost acquisition, display, and evaluation setup for tactile codec development. In: Proceedings of IEEE International Symposium on Haptic, Audio and Visual Environments and Games (HAVE), 2018. 1–6
- 38 Landin N, Romano J M, Mcmahan W, et al. Dimensional reduction of high-frequency accelerations for haptic rendering. In: Proceedings of EuroHaptics, 2010. 79–86
- 39 Zhang Q, Zhang S, Zhu X, et al. The haptic tele-operation system for Tactile Internet: architecture, challenges, and implementation. IEEE Netw, 2025, doi: 10.1109/MNET.2025.3534857
- Hassen R, Steinbach E. Subjective evaluation of the spectral temporal SIMilarity (ST-SIM) measure for vibrotactile quality assessment. IEEE Trans Haptics, 2020, 13: 25–31
- 41 Okamoto S, Konyo M, Saga S, et al. Detectability and perceptual consequences of delayed feedback in a vibrotactile texture display. IEEE Trans Haptics, 2009, 2: 73–84